15TH IEA HEAT PUMP CONFERENCE
MAY 26–29, 2026 | HOFBURG
VIENNA 2026
DECARBONISATION THROUGH INNOVATION

Investigation of high temperature packed bed TES system

Jungchul Kim[a,*] , Sunyoung Moon [a], Jinwoo Yoo[a], Sang Jin Park[a], Chan Ho Song [a]

[a] Heat Pump Research Center, Korea Institute of Machinergy & Materials, 156 Gaejeongbuk-Ro, Yuseung-Gu, Daejeon 34103, South Korea

Abstract

With the efficient use of energy becoming an increasingly significant environmental concern, interest in high-temperature thermal energy storage systems is growing. Thermal energy storage systems can be categorized into chemical heat storage, latent heat storage, and sensible heat storage. In this study, we focused on the sensible heat storage type due to its ability to stably store and release heat at high temperatures. Among sensible heat storage methods, the packed bed type and the block and pipe type are primarily used. We conducted research on the packed bed type, which offers advantages regarding the thermocline. To theoretically understand the fundamental thermal storage mechanism, we employed a 1-D model and derived the governing equations. Through numerical analysis, we examined the temperature profiles. To investigate parametric dependency, we analyzed changes in the temperature profiles by varying solid properties such as particle size, density, and specific heat, as well as fluid properties such as velocity, density, specific heat, and viscosity. Additionally, through a normalization process, we derived solutions that can be generally applied across various conditions.

© HPC2026.
Selection and/or peer-review under the responsibility of the organizers of the 15th IEA Heat Pump Conference 2026.

Keywords: Thermal energy storage; Thermocline; Packed bed system; Universal solution; Charge and discharge

1. Introduction

As carbon neutrality has become a primary societal value, interest in thermal energy is increasing. Consequently, there is growing attention towards the use of renewable energy and ultra-high temperature thermal energy storage (TES).

This research was conducted with a maximum temperature of 300 °C, and among the various TES methods, the sensible heat storage method was adopted. While packed bed and block and pipe types are primarily used for ultra-high temperature sensible heat storage, the packed bed type was initially selected due to its advantage in terms of the thermocline, and research was conducted on this topic.

To theoretically understand the fundamental heat storage mechanism, 1-D governing equations were derived [1-3]. Through numerical analysis, the temperature profile was confirmed. To investigate parametric dependency, changes in the temperature profile were observed by varying solid properties (such as particle size, density, and specific heat) and fluid properties (such as fluid velocity, density, specific heat, and viscosity).

Furthermore, a non-dimensionalization process was performed to derive a solution that could be commonly applied across various different conditions. The reliability of the theory was enhanced by comparing the theoretical results with experimental results.

* Corresponding author. Tel.: +82-42-868-7840 ; fax: +82-42-868-7338.
E-mail address: jungchulkim@kimm.re.kr.

2. Experimental setup

This thermal energy storage experiment is designed to evaluate the performance of a system that stores and recovers heat in a packed bed composed of 93% alumina balls, using high-temperature air as the heat transfer fluid. The storage medium consists of alumina balls with a diameter of 20 mm. These are contained within the storage section of the thermal storage tank, which has dimensions of 1×1×2.8 m^3. To minimize heat loss to the exterior and enhance experimental accuracy, the internal insulation design incorporates 400 mm of ceramic wool.

To precisely determine the temperature distribution inside the system and the heat exchange status between the fluid and the solid, thermocouples are installed in pairs at the same axial position (x). One thermocouple measures the temperature inside the storage material (alumina ball) to monitor the energy storage state of the solid medium, while the other measures the temperature outside the storage material (in the air flow path) to record the temperature of the air. This setup allows for the simultaneous analysis of the heat transfer characteristics between the two media.

Fig. 1 and 2 show schematic diagram of the TES loop and the photo of the system, respectively. The experiment is conducted in a consistent cycle, consisting of 6 hours of charging (heat storage) followed by 6 hours of discharging (heat recovery). The properties of the fluid and solid are listed in Table. 1

Table 1. Properties of fluid and solid

	Air	Alumina 93%
Density ρ (kg / m3)	1.184 (25 ℃)	3,600
	0.6153 (300 ℃)	
Specific heat, cp (J/kg-K)	1006.6 (25 ℃)	800
	1045.4 (300 ℃)	
Thermal conductivity, k (W/m-K)	0.02585 (25 ℃)	20
	0.04369 (300 ℃)	

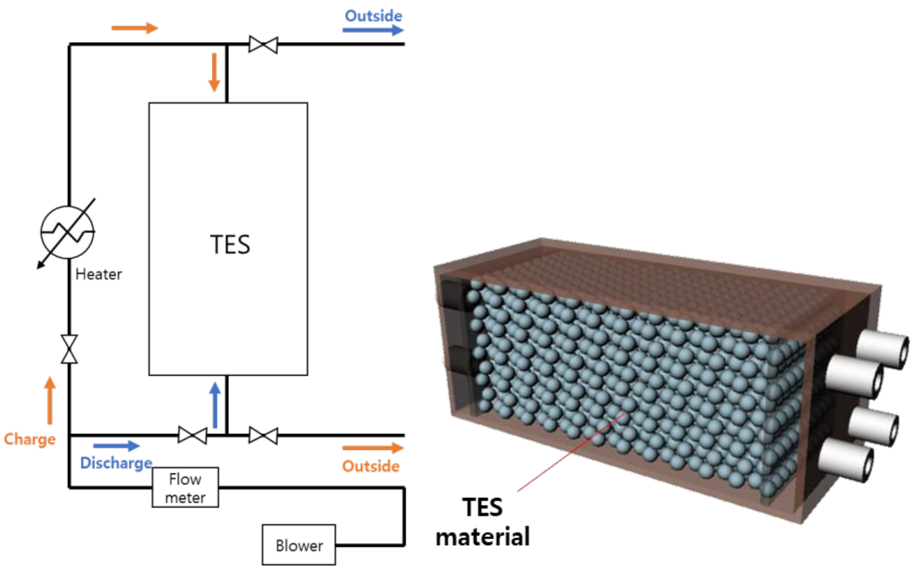

Figure 1. Schematic diagrams of TES system loop and TES chamber

Figure 2. Photo of TES system

3. Mathematical model and results

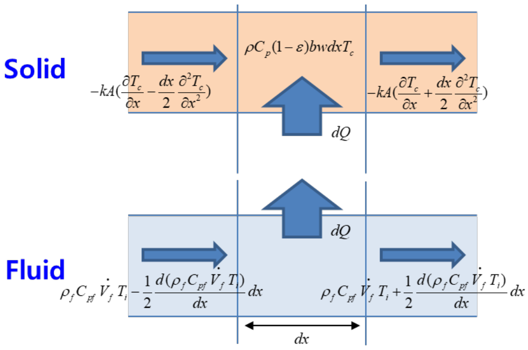

Figure 3. Heat transfer between TES material and working fluid

In this study, to understand the heat transfer mechanism of a fluid, we assumed a micro control volume and derived equations for the energy change within this control volume for both the solid phase and the fluid phase, based on the assumptions of heat transfer and fluid transfer across its boundaries. These equations are as follows.

$$\frac{dQ}{dx}\frac{1}{bw}\frac{1}{\varepsilon} = -u\frac{\partial(\rho_f C_{pf} T_f)}{\partial x} - \frac{\partial(\rho_f C_{pf} T_f)_t}{\partial t} \tag{1}$$

$$\frac{dQ}{dx}\frac{1}{bw}\frac{V_u}{1-\varepsilon} = -U(T_c - T_f)A_u \tag{2}$$

$$\frac{dQ}{dx}\frac{1}{bw}\frac{1}{1-\varepsilon} = \rho C_p\frac{\partial T_c}{\partial t} - Ck\frac{1}{1-\varepsilon}\frac{\partial^2 T_c}{\partial x^2} \tag{3}$$

The second term on the right-hand side of Equation (3) represents the conduction between particles. In the case of using spherical storage material in a packed bed, this value can be minimized because the particles form point contact. In this case, the constant C approaches zero, and this term can be effectively neglected.

The above governing equations can be expressed in a normalized form through a non-dimensionalization process. To this end, the non-dimensionalization factors were derived as follows.

$$T_f^* = \frac{T_f - T_{\min}}{T_{\max} - T_{\min}} \tag{4}$$

$$T_s^* = \frac{T_s - T_{min}}{T_{max} - T_{min}} \quad (5)$$

$$\eta = \frac{\rho_f c_{pf}}{\rho_s c_{ps}} \frac{\varepsilon}{1-\varepsilon} \quad (6)$$

$$Q^* = \frac{Q}{\rho_s c_{ps} \dot{V}_f (T_{max} - T_{min})} \frac{\varepsilon}{1-\varepsilon} \quad (7)$$

$$\tau = \frac{\rho_s c_{ps} V_u}{UA_u} \quad (8)$$

$$St = \frac{UA_u}{\rho_s c_{ps} u V_u} l = \frac{l}{u\tau} \quad (9)$$

$$x^* = \frac{x}{l} St = \frac{x}{u\tau} \quad (10)$$

$$t^* = \frac{u}{l} t \quad (11)$$

The governing equations in dimensionless form are written as follows,

$$\frac{dQ^*}{dx^*} = -\frac{\partial(\eta T_f^*)}{\partial x^*} - \frac{\partial(\eta T_f^*)}{\partial t^*} \quad (12)$$

$$\frac{dQ^*}{dx^*} = -T_s^* + T_f^* \quad (13)$$

$$\frac{dQ^*}{dx^*} = \frac{\partial T_s^*}{\partial t^*} \quad (14)$$

Table 2. Charging time of curves for all cases

Color	Black	Green	Magenta	Light blue (Cyan)
Material	Concrete	Concrete	Concrete	SUS 304 (k : Concrete)
D (m)	0.02	0.02	0.03	0.03
u (m/s)	0.02	0.1	0.02	0.02
t1 (h)	0.167	0.167	0.253	0.595
t2 (h)	1.5	1.5	2.287	5.373
t3 (h)	3	3	4.573	10.748
t4 (h)	6	6	9.148	21.495
t5 (h)	10	10	15.248	35.828
t6 (h)	13.334	13.334	20.331	47.77
t7 (h)	16.667	16.667	25.414	59.712
t8 (h)	20	20	30.495	71.656
t9 (h)	23.334	23.334	35.578	83.598
t10 (h)	30	30	45.745	107.484

The target storage materials, storage material size, fluid velocity, and time are shown in Table 2. The times are not all the same, as they are the times derived through the non-dimensionalization process mentioned above. Fig. 4 shows the numerical analysis results. Each case corresponds to conditions where the type of storage material, particle size, and velocity are varied.

The upper plot in Fig. 4 shows the temperature profiles according to the time and distance derived through non-dimensionalization. From this plot, it can be seen that the magenta and cyan points(curves) overlap perfectly. These two cases mean that the particle size of the storage material and the air velocity are exactly the same. That is, if these two are identical, the temperature profiles overlap perfectly for the time matched to the non-dimensional time t*. The lower graph is the x* and T* profile graph for the time matched to the non-dimensional time t*. The left and right graphs use different applied cases. First, the black, cyan, and green curves are the profiles for the same storage material. For the same type of storage material, the η in Equation (12) of the non-dimensional governing equations becomes the same, making the non-dimensional governing equations completely identical. In this situation, since they have the same solution regardless of velocity and particle size, all cases must necessarily overlap.

Following this principle, by using the non-dimensional time t*, x*, and T*, we can obtain the temperature profile for all spherical packed bed thermal energy storage devices that use air. For example, let's assume we want to find the temperature profile for a SUS 316 storage material with a velocity of 0.1 m/s and a storage material size of 0.05 m. First, we derive a representative temperature profile. Let's choose concrete with a size of 0.02 m and a velocity of 0.02 m/s. We first derive the upper plot of Fig. 4, ensuring that t* is matched. Since the upper graph of Fig. 4 matches when the velocity and unit storage material size are the same, the case for SUS 316 with 0.02 m and 0.02 m/s will completely coincide, allowing us to find the temperature profile for t*. Now, we use this value to find the graph for x* and T* (refer to the lower plots of Fig. 4). Since this graph perfectly coincides as long as the type of storage material is the same, this profile can be used to derive the temperature profile for the 0.05 m and 0.1 m/s case. In other words, if we know a reliable temperature profile for a known case, using the two graphs in Fig. 4 (using the governing equations and non-dimensional governing equations) allows us to derive the temperature profile for any case. In this regard, it can be said that we have derived a universal solution through the two governing equations mentioned above.

The experimental results are shown in Fig. 5. The charging capacity for 6hr is approximately 166 kWh and the charging/discharging efficiency about 90%.

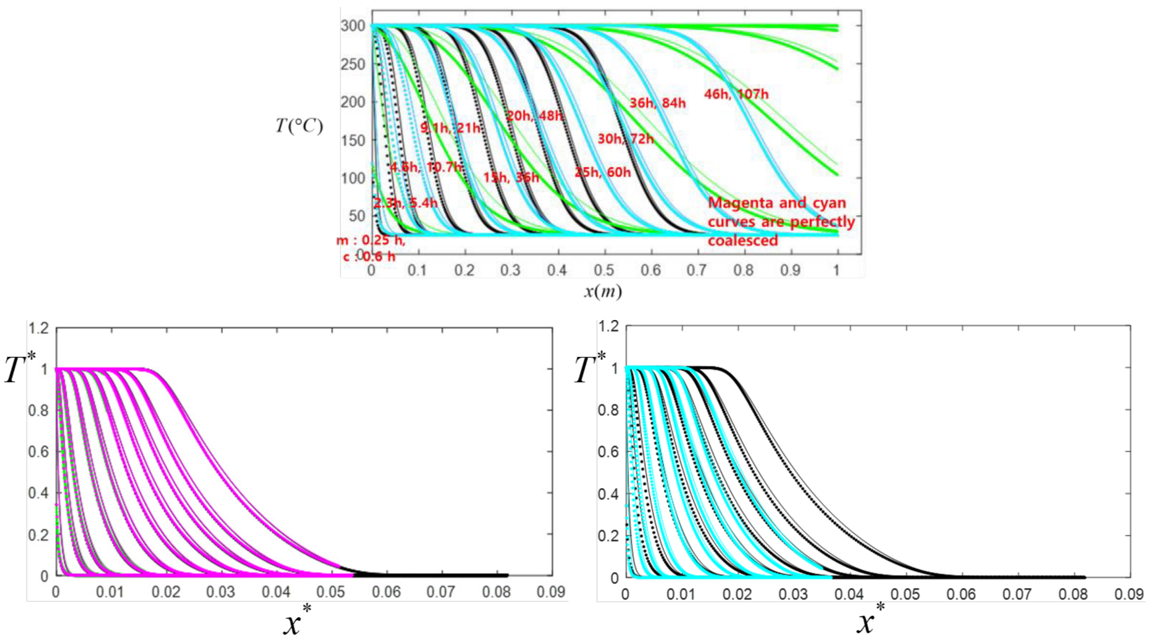

Figure 4. (Top) Temperature profiles for all cases, (Bottom left) for three cases except cyan dots (Bottom right), and for two cases, black and cyan dots, respectively.

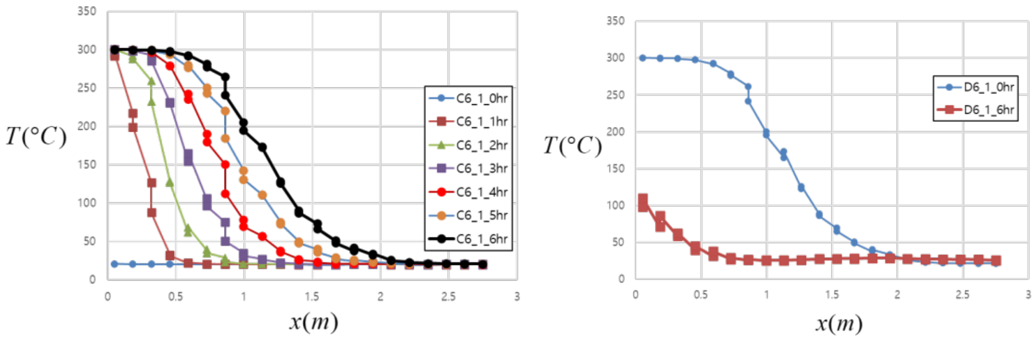

Figure 5. Temperature profiles of 6 hr charging/discharging experiments.

4. Conclusions

Through this study, we gained an understanding of the principles of heat and mass transfer in packed bed systems. By utilizing the fundamental heat and mass transfer equations along with the laws of energy and mass conservation, we derived the governing equations. Furthermore, through a non-dimensionalization process, we obtained a solution that can be broadly applied across various conditions.

Specifically, we found that by effectively utilizing the non-dimensional variables, if the fundamental assumptions are the same (negligible internal thermal conduction, Bi << 1 and the fluid is identical, one can easily derive the temperature profile for any other set of conditions, provided a single reliable profile is known.

Acknowledgements

This work was supported by Korea Institute of Machinery & Materials(NK262E).

References

[1] Hänchen M., Brückner S., and Steinfeld A. 2011, High-temperature thermal storage using a packed bed of rocks - Heat transfer analysis and experimental validation, Applied Thermal Engineering, Vol. 31, pp. 1798-1806.

[2] El Alami K., Asbik M., Zari N., and Rachidi S. 2018, Thermocline Thermal Storage Using a Packed bed of Moroccan Rocks, IOP Conference Series: Earth and Environmental Science, Vol. 161, pp. 012016.

[3] Alonso, E. and Rojas E. 2022, Air solid packed-beds for high temperature thermal storage: practical recommendations for predicting their thermal behaviour, Applied Thermal Engineering, Vol. 202, pp. 117835.